HHS Public Access

Author manuscript

Surgery. Author manuscript; available in PMC 2019 October 01.

Published in final edited form as:

Surgery. 2018 October ; 164(4): 909–915. doi:10.1016/j.surg.2018.06.017.

Disseminated Injection Of Vincristine-Loaded Silk Gel Improves The Suppression Of Neuroblastoma Tumor Growth

Jasmine Zeki, BS[1,*], **Jordan S. Taylor, MD**[1,*], **Burcin Yavuz, PhD**[2], **Jeannine Coburn, PhD**[2,3], **Naohiko Ikegaki, PhD**[4], **David L. Kaplan, PhD**[2], and **Bill Chiu, MD**[1,†]

[1]Department of Surgery, Stanford University, Stanford, CA

[2]Department of Biomedical Engineering, Tufts University, Medford, MA

[3]Department of Biomedical Engineering, Worcester Polytechnic Institute, Worcester, MA

[4]Department of Anatomy and Cell Biology, University of Illinois at Chicago, Chicago, IL

Abstract

Purpose—Advanced stage neuroblastoma patients require multi-agent chemotherapy. Intra-tumoral implantation of vincristine-loaded silk gel utilizes local diffusion to decrease orthotopic neuroblastoma tumor growth in mice. We hypothesize that injecting vincristine-loaded silk gel into eight locations within the tumor, instead of only centrally, decreases the diffusion distance and improves tumor growth suppression.

Methods—Human neuroblastoma cells, KELLY, were injected into mouse adrenal glands to create orthotopic tumors. After the tumors reached 100mm^3 by ultrasound, silk gels loaded with 50μg vincristine were injected centrally or in eight areas throughout the tumor. Drug-release profile was measured in vitro. Endpoints were tumor size>1000mm^3 and histologic examination.

Results—Vincristine-loaded silk gels suppressed tumor growth up to an “inflection point” (458.7±234.4mm^3 for central, 514.3±165.8mm^3 for eight-point injection) before tumor growth accelerated >200mm^3 over 3 days. The time to inflection point was 6.6days for central; 13.3days for eight-point injection($p<0.05$). Using the sphere volume equation $V = {}^4\!/_3\,\pi r^3$ to approximate tumor volume, splitting the volume into 1/8 decreased the diffusion radius by 1/2. Histology confirmed tumor necrosis adjacent to vincristine-loaded silk gel.

†To whom correspondence should be addressed: Bill Chiu, M.D., Department of Surgery - Pediatric Surgery, 300 Pasteur Drive, Always Building M116, Stanford University, Stanford, CA 94305, USA, Phone: (650) 723 – 6439, Fax: (650) 725 – 5577, bhsc@stanford.edu.

*Authors contributed equally to the work.

Presentation at Central Surgical Association 2018 Annual Meeting

March 15–17, 2018

Columbus, Ohio

Conclusions—Injecting vincristine-loaded sustained release silk gel at eight separate locations halved the diffusion distance and doubled the time for the tumor to reach the growth inflexion point.

Keywords

neuroblastoma; controlled release; vincristine; silk gel

INTRODUCTION

Neuroblastoma is the most common intra-abdominal solid tumor affecting children; it has a remarkably heterogeneous clinical presentations and accounts for 15% of all pediatric cancer related deaths (1, 2). While the mainstay treatment for low-risk disease is surgical resection (3), patients with high-risk disease are treated with an aggressive, multimodal approach. Multi-agent systemic chemotherapy can include doxorubicin, vincristine, cyclophosphamide, cisplatin, topotecan, and etoposide (2). Despite advances in surgical techniques, chemotherapy, radiotherapy, and immunotherapy, survival rate for children with advanced-stage neuroblastoma is still under 50% (4). Furthermore, toxicity from systemic chemotherapy results in significant patient morbidity including renal toxicity, myelosuppression, cardiotoxicity, and long-term complications including secondary malignancy (5).

The development of novel drug delivery systems that can maximize tumor cell death and minimize systemic side effects is essential for improving outcomes for pediatric patients (6–8). We previously utilized sustained release silk delivery platforms to treat orthotopic neuroblastoma mouse xenografts by implanting the platform into the center of the tumor (9). This treatment strategy resulted in significant decreases in tumor growth as well as reductions in systemic toxicity compared to delivering the same dose intravenously.

Using our orthotopic neuroblastoma xenograft model (9), we aimed to improve tumor growth suppression by altering the diffusion parameters. We engineered sustained release silk gels loaded with vincristine that were injected either centrally or throughout the tumor. We hypothesized that tumor growth would be more significantly suppressed by distributed injections compared to central injections of vincristine-loaded silk gel, as a consequence of decreased diffusion distances.

METHODS

Silk fibroin extract

Silk fibroin from *Bombyx mori* silkworm cocoons was extracted as previously described (10). Briefly, cocoons were cut into approximate 1 cm^2 pieces and boiled in 0.02 M $NaCO_3$ for 30 minutes to extract the sericin protein. The silk fibroin fibers were dried overnight and then dissolved in 9.3 M LiBr solution for 3 hrs at 60°C. The silk fibroin solution was then dialyzed (3.4 kDa MWCO dialysis cassettes, Thermo Fisher Scientific, Waltham, MA) against ultrapure water at room temperature for two days with seven water changes resulting

in an approximately 6.5% (w/v) aqueous silk fibroin solution. The silk fibroin solution was stored at 4°C for later use.

Vincristine-loaded silk gel

Silk fibroin gel was prepared as previously described (9). Briefly, the silk solution as described above was sterile filtered. Then two mL of the prepared solution was sonicated using a Branson Digital Sonifier 450 (Branson Ultrasonics, Danbury, CT) at 10% amplitude for 15 sec and placed on ice for 2 min and sonicated one additional time. Twenty microliters of the pregelled solution was aspirated into a 0.5 mL insulin syringe and allowed to gel at 60°C. A solution of 60 min extracted silk was prepared at 6.85% (w/v) and sterile filtered. Two milliliters of the prepared solution was sonicated at 15% amplitude for 30 sec and placed on ice. Vincristine from a 5 mg/mL (125μL) stock was added to the pre-gelled silk solution (875μL) to achieve a final concentration of 625 μg/mL vincristine and 6% (w/v) silk. Eighty microliters of the vincristine-loaded pre-gel was aspirated into the previously prepared syringes and allowed to gel at room temperature overnight. The final vincristine amount was 50 μg per syringe; the total dose of injected vincristine was 50 μg per mouse in the treatment groups.

Vincristine release characterization

In vitro release studies were performed under sink conditions where *"the volume of medium at least ten times that required in order to form a saturated solution of drug substance"* (11). Vincristine-loaded drug delivery systems were placed into 1 mL of phosphate buffered saline (PBS, pH 7.4 Life Technologies, Grand Island, NY) at 37°C for release quantification. At each time point, the PBS was completely removed and replaced with fresh PBS. The drug concentration was determined via Ultraviolet/visible (UV/Vis) light spectroscopy (SpectraMax M2 spectrophotometer; Molecular Devices, Sunnyvale, CA). A standard curve for vincristine using an absorbance wavelength of 298 nm was generated to determine the vincristine concentration within the release medium. Blank gel samples were used for control readings.

Cell culture

Human neuroblastoma KELLY cells (Sigma-Aldrich, St Louis, MO) were maintained in RPMI 1640 (HyClone, Logan, UT) supplemented with 10% fetal bovine serum, 100 IU/ml penicillin, 100 μg/ml streptomycin, and 2 mM glutamine. All cells were maintained in a 5% CO_2 atmosphere at 37°C and trypsin-passaged at 80% confluence.

Mouse orthotopic neuroblastoma model

All mouse procedures were performed in accordance with the National Institute of Health protocols on Humane Care and Use of Laboratory Animals and approved by the Institutional Animal Care and Use Committee. The establishment of orthotopic neuroblastoma xenograft in a seven-week old female NCr nude mouse (Harlan, Indianapolis, IN, USA) was previously described (9). Briefly, the mouse was anesthetized with inhalational isoflurane. A transverse incision was made on the left flank to locate the left adrenal gland, and 2 μL of phosphate buffered saline (PBS) containing one million KELLY cells were injected into the

adrenal gland. The fascia and skin were closed in separate layers. Tumor formation was followed by non-invasive ultrasound measurements, and the animals euthanized when the tumor volume exceeded 1000mm^3. The tumor was harvested, embedded in paraffin, and sectioned for immunohistochemical staining with heamatoxylin and eosin (H/E), Ki67, and TUNEL assay.

High frequency ultrasound

After anesthetizing with inhalational isoflurane, the mouse was secured in a prone position, and a VisualSonics Vevo 2100 sonographic probe (Toronto, Ontario, Canada) was placed over the left flank to locate the left adrenal gland and the tumor. Serial cross-sectional images (0.076 mm between images) were taken, and 3-D reconstruction tool (Vevo Software v1.6.0, Toronto, Ontario, Canada) was used to calculate the tumor volume.

Injection of vincristine-loaded silk fibroin gel into orthotopic neuroblastoma tumor

After the orthotopic neuroblastoma tumor reached 100mm^3 by ultrasound, the mice were briefly anesthetized with inhaled isoflurane. Previous skin and fascial incisions were re-opened to gain direct access to the adrenal gland/tumor. Sustained release silk gel loaded with 50 μg of vincristine was injected into the tumor in either a single, central injection or distributed-injection pattern consisting of eight points (Figure 1) using a 28G insulin needle. Control mice with size matched tumors were injected with silk gel not loaded with any drug either centrally or in the eight point distributed pattern. The fascia and skin were closed in separate layers. Tumor formation was followed by non-invasive ultrasound measurements, and the animals euthanized when the tumor volume exceeded 1000mm^3.

Statistical analysis

Tumor sizes and post-operative days were entered into a scatter plot, and a curve of best fit with the associated equation was created for each animal. By entering the desired tumor size (500mm^3, 600 mm^3, 700 mm^3, or 800 mm^3) into the equation, we solved for the post-operative day using the “goal seek” function under the “what-if analysis” (Microsoft Excel, 2011, version 14.7.4, Redmond, Washington). The post-operative days obtained were compared between different groups using Student’s t test, and a p value <0.05 was considered statistically significant. Cell death and proliferation were quantified by counting TUNEL and Ki67 positive cells per area on representative slides. Quantified cell death and proliferation among the groups were compared using Studen’s t test and a p value <0.05 was considered statistically significant.

RESULTS

Drug release from silk gel

The amount of drug released from silk gel loaded with 50 μg of vincristine was measured in vitro (Figure 2). The platform released 5.61 ± 2.49 μg of vincristine at two hours, 3.13 ± 1.36 μg at five hours, followed by an additional 5.11 ± 1.94 μg at 24 hours; 1.78 ± 0.46 μg on day 3; 0.82 ± 0.82 μg on day 7; 0.37 ± 0.48 μg on day 10; 0.14 ± 0.32 μg on day 14, and 0.77 ± 0.59 μg on day 22. The initial release on day one accounted for 27.70 ± 3.88 % of the

total drug loaded, with a more gradual release of vincristine after day 3–5. Nearly half (49.82 ± 1.82 %) of the total vincristine amount was released in vitro by day 32.

Tumor growth

Neuroblastoma tumor injected with silk gel loaded with vincristine 50 μg at the center had decreased tumor growth compared to control gel (without drug) injected at the center ($p<0.05$). Tumor size reached 500mm^3 in 7.3 ± 3.3 days vs 0.3 ± 0.9 days ($p = 0.02$); tumor reached 600mm^3 in 8.6 ± 3.7 days vs 0.9 ± 1.1 days ($p = 0.02$); tumor reached 700mm^3 in 9.8 ± 4.1 days vs 1.4 ± 1.2 days ($p = 0.02$); and tumor reached 800mm^3 in 11 ± 4.4 days vs 2 ± 1.4 days ($p = 0.02$), respectively (Figure 3A).

Neuroblastoma tumor injected with silk gel loaded with vincristine 50 μg total at eight separate locations within the tumor had decreased tumor growth compared to control gel injected at eight different locations within the tumor ($p<0.05$): tumor size reached 500mm^3 in 8.7 ± 3.7 days vs 0.7 ± 0.2 days ($p = 0.02$); tumor reached 600mm^3 in 10.2 ± 3.8 days vs 1.6 ± 02 days ($p = 0.02$); reached 700mm^3 in 11.6 ± 3.9 days vs 26 ± 0.3 days ($p = 0.02$); and tumor reached 800mm^3 in 12.9 ± 3.9 days vs 3.5 ± 0.4 days ($p = 0.01$), respectively (Figure 3B).

Control tumors, treated with silk gel not loaded with any drug either centrally or in the distributed injection pattern showed similar growth patterns. There was no significant difference in the time for the control tumors to reach 500mm^3, 600mm^3, 700mm^3, or 800mm^3 based on the injection pattern ($p = 0.5$, 0.29, 0.20, and 0.15, respectively). There was no evidence of bleeding or disruption of the blood supply immediately after injection, regardless of injection pattern.

Tumors treated with silk gel loaded with vincristine 50 μg either centrally (n = five mice) or divided into eight separate locations (n = six mice) within the tumor appeared to have a perod of minimal growth (<200mm^3 over three days) followed by an increased rate of tumor growth (>200mm^3 over three days). We defined the transition between these two growth patterns as the “inflexion point”. The inflexion point for the centrally-treated tumors was at 6.6 ± 4.1 days after treatment; tumors treated at eight locations reached the inflection point at 13.3 ± 3.9 days ($p<0.05$) (Figure 4). The tumor size at the inflection point was similar for both groups; 514.3 ± 165.8 mm^3 for the centrally-treated tumors and 458.7 ± 234.4 mm^3 for the eight point-treated tumors.

Histology

Mice were sacrificed after tumor volume reached >1000mm^3 by ultrasound and tumors treated with vincristine-loaded or control gel either centrally or at eight different locations (Figure 1) were embedded in paraffin, sectioned, and stained with H/E, Ki67, or TUNEL (Figure 5). H/E staining of tumor cells adjacent to the vincristine-loaded silk gel showed tumor necrosis which was not observed in tumor cells adjacent to the control gel (Figure 5A and 5B). Both vincristine-loaded and control gel treated tumors showed viable and typical small-round-blue cells (SBRC) of neuroblastoma. The Ki67 staining, a marker for proliferation, was positive, and the TUNEL assay showed minimal apoptosis in the post-inflection point tumors (Figure 5C). Since the tumors were harvested when the tumor size

reached >1000mm^3, all groups showed similar proportions of viable and apoptotic tumor cells (Figure 5C). Vincristine-treated specimens had 252 ± 78 TUNEL-positive cells/mm^2 in the eight-point injection model compared to 185 ± 31 TUNEL-positive cells/mm^2 in the center injection model ($p = 0.238$). There was no significant difference in the TUNEL-positive cells/mm^2 when comparing both vincristine groups with control groups (219 ± 64 vs 193 ± 81 cells/mm^2, respectively; $p = 0.559$). The amount of proliferation by Ki67-positive cells/mm^2 was also similar between all groups: 6393 ± 1073 cells/mm^2 in the vincristine-treated groups compared to 6715 ± 446 cells/mm^2 in the control groups ($p = 0.514$).

DISCUSSION

We have loaded vincristine into sustained release silk gels and injected these materials within an orthotopic neuroblastoma tumor. Using this approach, we were able to decrease the tumor growth rate. In particular, injecting the equivalent total dose vincristine-loaded gel separately at eight different locations within the tumor was superior to injecting the gel centrally, doubling the time to reach the inflexion point. Furthermore, assuming vincristine diffused over a spherical space from the gel, injecting vincristine-loaded silk gel at eight different locations within the tumor in effect split the total tumor volume by 1/8 and halved the diffusion radius ($V = {}^4\!/_3 \pi r^3$). The histologic examination by H/E demonstrated that tumor cell necrosis contributed to the decrease in tumor growth rate.

This study took advantage of observed tumor growth patterns. Orthotopic tumors, regardless of the drug delivery method, grew initially at a slow rate until the tumor mass reached a critical point. After this point, which we defined as the inflection point, tumor growth rate expanded to >200mm^3 over three days. This enabled us to see tumor responses to therapy at an earlier stage and thereby, not have to rely on survival statistics. Our results showed a doubling in the time for the tumor to reach its inflection point when the tumor volume was treated by eight separate injections. The inflection point provided an additional variable along with tumor size that could be used to judge therapeutic response.

There was no significant difference on histologic exam in the number of Ki67-positive or TUNEL-positive cells between either control or vincristine-treated groups, regardless of injection pattern. In order for the growth kinetics to be evaluated, the histologic exam was performed after the tumors reached 1000mm^3, long after the difference in growth rate was observed. The tumors exhibited a differential growth pattern initially, but given enough time, the tumors continue to grow through this intermediate dose of vincristine, yielding comparable histologic and immunostaining results one might expect with viable tumor.

Vincristine dose of 50 μg was chosen based on previous work, which demonstrated tumor growth suppression (12). We previously demonstrated higher concentrations of vincristine-loaded silk-based platforms could suppress tumor growth for up to 150 days (9). Higher doses of vincristine were also associated with more side effects. We chose an intermediate dose that could still suppress tumor growth on a more feasable time scale and demonstrate the benefits of a distributed injection model. Furthermore, this dose of vincristine implanted intra-tumoraly has been shown to yield higher intra-tumor drug concentrations and lower

plasma drug concentrations than 50 μg vincristine administered intravenously (9). The prior work supports the argument that local therapy can improve treatment outcomes by increasing the effect on the tumor while decreasing systemic toxicity.

KELLY cells were used to generate orthotopic tumor models based on previous work (8) that demonstrated more rapid growth compared to other MYCN amplified and nonamplified lines. Durg-loaded sustained release silk platforms were effective at decreasing tumor growth in all tested tumor lines; however, the KELLY orthotopic tumor model was chosen in this study as the most appropriate model for locally advanced tumors, given its aggressive growth.

We have previously loaded vincristine onto other sustained release platforms, such as a silk wafer (13). The silk gel represents a more versatile format in application, simply injecting through a needle. Although we accessed the tumors via an open incision, the distributed method of injecting drug-loaded silk gel could be easily adapted to a less invasive procedure. The potential advantage is even greater for pediatric patients, who could undergo sonographic or CT-guided techniques to percutaneously inject drug-loaded silk gel with light sedation. These radiological modalities can also be used to estimate tumor volume, and in combination with the drug release profile of the sustained release platform, the tumor response can be predicted (12). This intra-tumoral sustained release approach can be further extended to include loading more than one chemotherapeutic drug, thus increasing the tumor cell death (9). As the drug was applied within the tumor, the resultant toxicity was more favorable than administering the drug intravenously (9).

Intra-tumoral implantation of drug-loaded sustained release platform relies on diffusion for the drug to reach the tumor cells. Fick's law of diffusion, the same law that governs pulmonary gas exchange and can be used to calculate cardiac output, states that flux, F, is proportional to the concentration gradient, C, over a distance, *x*, and the diffusion coefficient, D: $F = -D\frac{\partial C}{\partial x}$ (14, 15). Drug delivery platforms is an active area of research, where configurations and delivery reservoirs are modeled and modified to improve release profiles (15). The advantage of our model, however, depends on decreasing the diffusion distance by augmenting the geometry, not by changing the properties of the delivery platform. The additional injections using a small gauge needle did not contribute to the difference in growth (i.e. by causing more bleeding or tissue damage), as evident by the similar growth patterns of the control groups, regardless of the injection pattern. The result is slower tumor growth in a model that could be applicable with various (or multiple) drugs and platforms. While our eight-point injection model was chosen for its ease of application based on a spherical tumor, the optimal pattern of injection could be different based on the initial geometry of the tumor.

There are few clinically used drug delivery systems, Norplant® and Implanon™, where drug diffuses from an implanted reservoir (16). These implantable systems require a subsequent procedure for removal (17, 18). Silk fibroin, however, degrades via an enzymatic reaction to peptides and amino acids, eliminating the need for subsequent removal procedures (19). Silk fibroin-based material has been examined in numerous animal models, and found to have minimal immunologic response and favorable degradation properties (20–22). This

distributed injection model could foreseeably be used to improve local drug delivery systems, as an alternative to neo-adjuvant therapy for unresectable disease or as an adjunct to surgery when complete resection is not feasible.

Our previous work has shown that chemotherapy-loaded sustained release silk platforms can achieve tumor growth suppression when implanted within the tumor (9). By modifying the method of delivery to a distributed pattern throughout the tumor, we have shown that we can improve tumor growth suppression by decreasing the diffusion distance. Future work will focus on modeling the optimal distribution pattern for sustained release silk gel injections, testing the effect of distributive injections using multiple chemotherapeutic agents, and transitioning this technique to a minimally invasive approach that can potentially be used clinically.

Acknowledgments

This work was supported by the National Institutes of Health grants R01NS094218 (to D.L.K. and B.C.), P41EB002520 (to D.L.K.), and F32DK098877 (to J.M.C.).

References

1. Pizzo PA, Poplack DG. Principles and practice of pediatric oncology. Lippincott Williams & Wilkins; 2015.
2. Maris JM, Hogarty MD, Bagatell R, Cohn SL. Neuroblastoma. The Lancet. 369(9579):2106–20.
3. De Bernardi B, Mosseri V, Rubie H, Castel V, Foot A, Ladenstein R, et al. Treatment of localised resectable neuroblastoma. Results of the LNESG1 study by the SIOP Europe Neuroblastoma Group. British journal of cancer. 2008; 99(7):1027. [PubMed: 18766186]
4. Whittle SB, Smith V, Doherty E, Zhao S, McCarty S, Zage PE. Overview and recent advances in the treatment of neuroblastoma. Expert review of anticancer therapy. 2017; 17(4):369–86. [PubMed: 28142287]
5. Baker DL, Schmidt ML, Cohn SL, Maris JM, London WB, Buxton A, et al. Outcome after Reduced Chemotherapy for Intermediate-Risk Neuroblastoma. New England Journal of Medicine. 2010; 363(14):1313–23. [PubMed: 20879880]
6. Harris J, Chiu B. Clinical Considerations of Focal Drug Delivery In Cancer Treatment. Current drug delivery. 2017
7. Seib FP, Coburn J, Konrad I, Klebanov N, Jones GT, Blackwood B, et al. Focal therapy of neuroblastoma using silk films to deliver kinase and chemotherapeutic agents in vivo. Acta biomaterialia. 2015; 20:32–8. [PubMed: 25861948]
8. Chiu B, Coburn J, Pilichowska M, Holcroft C, Seib F, Charest A, et al. Surgery combined with controlled-release doxorubicin silk films as a treatment strategy in an orthotopic neuroblastoma mouse model. British journal of cancer. 2014; 111(4):708–15. [PubMed: 24921912]
9. Coburn J, Harris J, Zakharov AD, Poirier J, Ikegaki N, Kajdacsy-Balla A, et al. Implantable chemotherapy-loaded silk protein materials for neuroblastoma treatment. International journal of cancer. 2017; 140(3):726–35. [PubMed: 27770551]
10. Rockwood DN, Preda RC, Yucel T, Wang X, Lovett ML, Kaplan DL. Materials fabrication from Bombyx mori silk fibroin. Nature Protocols. 2011; 6(10):1612–31. [PubMed: 21959241]
11. Phillips DJ, Pygall SR, Cooper VB, Mann JC. Overcoming sink limitations in dissolution testing: a review of traditional methods and the potential utility of biphasic systems. Journal of Pharmacy and Pharmacology. 2012; 64(11):1549–59. [PubMed: 23058042]
12. Coburn JM, Harris J, Cunningham R, Zeki J, Kaplan DL, Chiu B. Manipulation of variables in local controlled release vincristine treatment in neuroblastoma. Journal of pediatric surgery. 2017; 52(12):2061–5. [PubMed: 28927981]

13. Harris JC, Coburn JM, Kajdacsy-Balla A, Kaplan DL, Chiu B. Sustained delivery of vincristine inside an orthotopic mouse sarcoma model decreases tumor growth. Journal of pediatric surgery. 2016; 51(12):2058–62. [PubMed: 27680598]
14. Crank J. The mathematics of diffusion. Oxford university press; 1979.
15. Siepmann J, Siepmann F. Modeling of diffusion controlled drug delivery. Journal of Controlled Release. 2012; 161(2):351–62. [PubMed: 22019555]
16. Pritchard EM, Szybala C, Boison D, Kaplan DL. Silk fibroin encapsulated powder reservoirs for sustained release of adenosine. Journal of Controlled Release. 2010; 144(2):159–67. [PubMed: 20138938]
17. Wu CJ, Wu XR, Xia WJ, Li RL. Study on in vivo release of levonorgestrel-containing silicon capsule. Journal of Tongji Medical University = Tong ji yi ke da xue xue bao. 1995; 15(3):167–70. [PubMed: 8731947]
18. Major I, Fuenmayor E, McConville C. The Production of Solid Dosage Forms from Non-Degradable Polymers. Current pharmaceutical design. 2016; 22(19):2738–60. [PubMed: 26898737]
19. Brown J, Lu CL, Coburn J, Kaplan DL. Impact of silk biomaterial structure on proteolysis. Acta Biomaterialia. 2015; 11:212–21. [PubMed: 25240984]
20. Wang Y, Rudym DD, Walsh A, Abrahamsen L, Kim HJ, Kim HS, et al. In vivo degradation of three-dimensional silk fibroin scaffolds. Biomaterials. 2008; 29(24–25):3415–28. [PubMed: 18502501]
21. Horan RL, Antle K, Collette AL, Wang Y, Huang J, Moreau JE, et al. In vitro degradation of silk fibroin. Biomaterials. 2005; 26(17):3385–93. [PubMed: 15621227]
22. Kim JH, Park CH, Lee OJ, Lee JM, Kim JW, Park YH, et al. Preparation and in vivo degradation of controlled biodegradability of electrospun silk fibroin nanofiber mats. Journal of biomedical materials research Part A. 2012; 100(12):3287–95. [PubMed: 22733605]

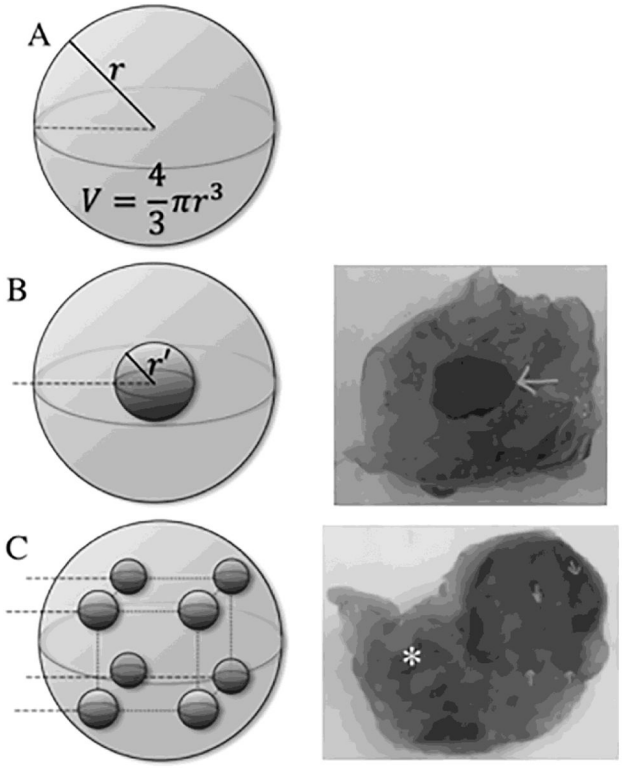

Figure 1.

Single intra-tumor administration of vincristine-loaded silk gel vs distributed injection, schematic and gross sections. **(A)** Spherical representation of tumor, r = radius, Volume = $4/3\pi r^3$. **(B)** Single injection into the center of tumor, r′ = radius of silk gel deposit; diffusion distance = r − r′. **(C)** Distributed injection into tumor at eight points using four passes with two silk gel deposits at each pass. Arrow (→): sites of gel deposit on gross specimen; astrisk (*): left kidney; dotted line: injection pass.

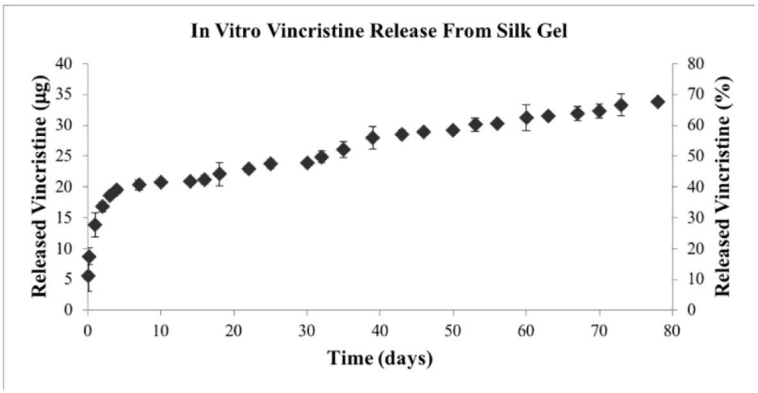

Figure 2.

Vincristine 50 µg release from silk gels in vitro, showing cumulative release of drug in µg and in percentage of total drug released. Error bars represent one standard deviation.

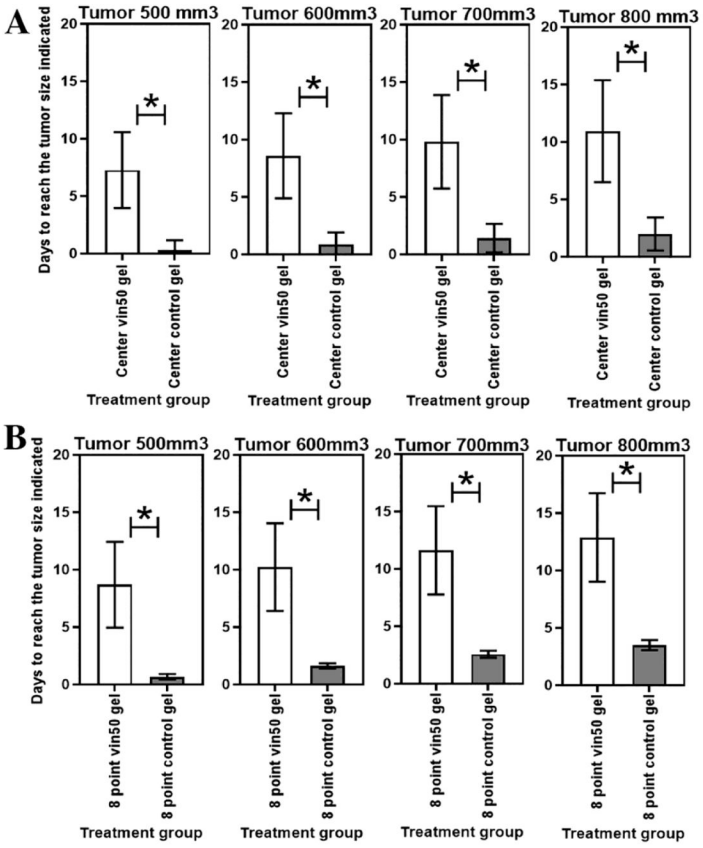

Figure 3.

Control gel vs vincristine-loaded gel. Time for tumor to reach 500mm^3, 600 mm^3, 700 mm^3, or 800 mm^3 comparing **(A)** central injection with vincristine 50 μg vs control; **(B)** eight-point injection of vincristine 50 μg vs control. Error bars represent one standard deviation; astrisk (*) indicates $p < 0.05$.

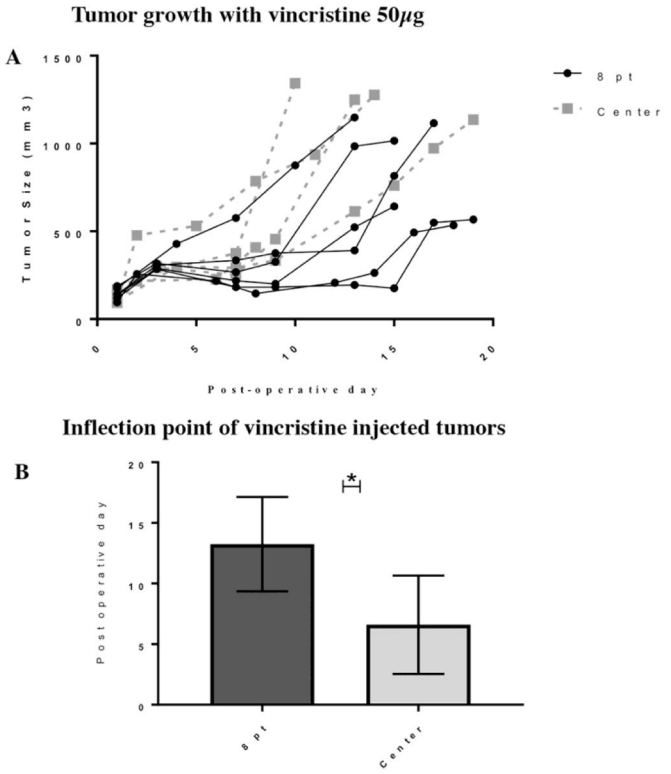

Figure 4.

(A) Tumor growth curve for neuroblastoma treated with eight-point injection or central injection of vincristine-loaded silk gel. **(B)** Inflection point for tumors was reached at 13.3 days for eight-point injection and 6.3 days for single injection ($p < 0.05$). Error bars represent one standard deviation; asterisk (*) indicates $p<0.05$.

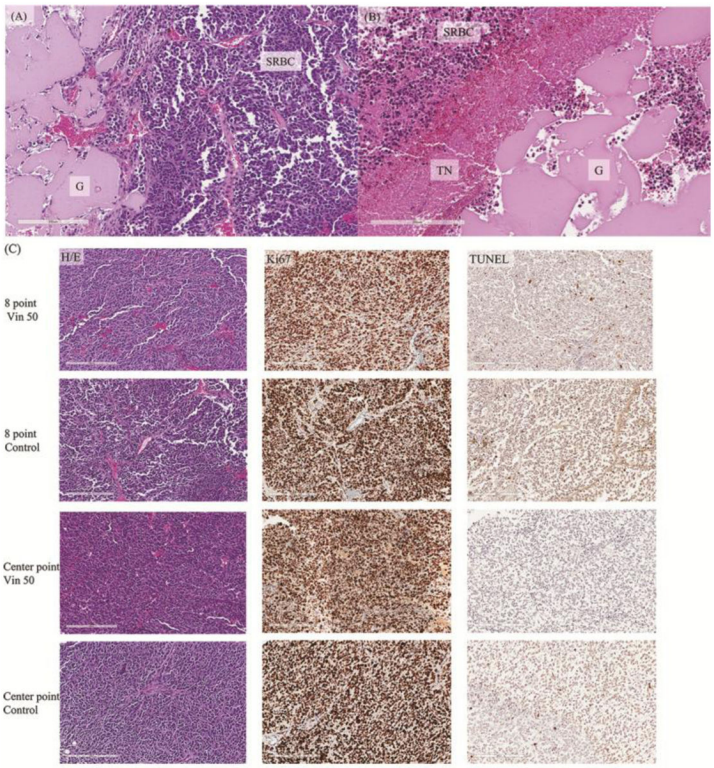

Figure 5.

(A) Heamatoxylin and eosin (H/E) staining of paraffin embedded neuroblastoma tumor section adjacent to injected control silk gel without drug. Viable cells were presents adjacent to the gel. **(B)** H/E staing of paraffin embedded neuroblastoma tumor section adjacent to vincristine-loaded silk gel. An area of tumor cell necrosis was adjacent to the drug-loaded silk gel. Beyond the area of tumor cell necrosis were viable tumor cells. **(C)** Immunohistochemical staining of paraffin embedded tumor sections using H/E, Ki67, and TUNEL at the time of sacrification. H/E staining showed small round blue cells of neuroblastoma tumor; Ki67 staining showed the multitude of proliferating tumor cells; TUNEL assay demonstrated minimal apoptosis in these tumors that have grown beyond their inflection point. G: silk gel, SRBC: small round blue cells of viable neuroblastoma cells, TN: tumor necrosis, Vin: vincristine.